

Metal forming analysis using meshfree-enriched finite element method and mortar contact algorithm

Wei Hu* and C.T. Wu^a

Livermore Software Technology Corporation, 7374 Las Positas Road, Livermore, CA 94551, USA

(Received March 2, 2013, Revised April 3, 2013, Accepted May 6, 2013)

Abstract. In this paper, a meshfree-enriched finite element method (ME-FEM) is introduced for the large deformation analysis of nonlinear path-dependent problems involving contact. In linear ME-FEM, the element formulation is established by introducing a meshfree convex approximation into the linear triangular element in 2D and linear tetrahedron element in 3D along with an enriched meshfree node. In nonlinear formulation, the area-weighted smoothing scheme for deformation gradient is then developed in conjunction with the meshfree-enriched element interpolation functions to yield a discrete divergence-free property at the integration points, which is essential to enhance the stress calculation in the stage of plastic deformation. A modified variational formulation using the smoothed deformation gradient is developed for path-dependent material analysis. In the industrial metal forming problems, the mortar contact algorithm is implemented in the explicit formulation. Since the meshfree-enriched element shape functions are constructed using the meshfree convex approximation, they pose the desired Kronecker-delta property at the element edge thus requires no special treatments in the enforcement of essential boundary condition as well as the contact conditions. As a result, this approach can be easily incorporated into a conventional displacement-based finite element code. Two elasto-plastic problems are studied and the numerical results indicated that ME-FEM is capable of delivering a volumetric locking-free and pressure oscillation-free solutions for the large deformation problems in metal forming analysis.

Keywords: meshfree; finite element; nonlinear; near-incompressible; plasticity; contact

1. Introduction

Metals are typical examples with nearly incompressible material behavior: isochoricity of the plastic deformation presents incompressibility constraints in metal plasticity. On the other hand, metals often experience excessive strains in the practice which could be in the order of several hundred percent in forging and extrusion analysis. The incompressibility constraints and large material deformation have presented tremendous difficulties in the numerical simulation using the standard displacement-based finite element formulation.

The incompressible locking in finite element methods has been studied extensively and many special numerical techniques have been proposed to resolve this difficulty. Among them are reduced/selective integration (Hughes 2000), reduced integration and hourglass control method

*Corresponding author, Professor, E-mail: whu@lstc.com

^a Ph.D., E-mail: ctwu@lstc.com

(Belytschko *et al.* 2001), Taylor expansion method (Liu *et al.* 1986), mixed formulation (Zienkiewicz and Taylor 1987), pressure projection method (Chen *et al.* 1996) and average nodal pressure element (Bonet and Burton 1998). The approach based on mixed formulation has a close link with Hughes's reduced/selective integration (Malkus and Hughes 1978) where the displacement and pressure interpolant spaces are subjected to an inf-sup condition (Babuska 1973) for the stability requirement. In Taylor expansion method, an assumed strain field (Simo and Hughes 1986) is obtained by the Taylor expansion of displacement gradient matrix and the resulting discrete equation can be expressed explicitly by one-point quadrature terms and their stabilization (Liu *et al.* 1986). In pressure projection method, the pressure computed from the displacement field is projected onto a lower-order space by a least-squares projection at the element level. The resulting equilibrium equation is equivalent to the perturbed Lagrangian formulation (Chen *et al.* 1997). Since the pioneering work (Bonet and Burton 1998), various average nodal pressure formulations (Andrade Pires *et al.* 2004, Krysl and Zhu 2008) have been developed to overcome incompressible locking. A priori error estimate (Lamichhane 2009) using primal and dual meshes reveals that original average nodal pressure formulation does not satisfy a uniform inf-sup condition (Babuska 1973). In order to have a stable formulation, the linear displacement space needs to be enriched with bubble functions as in the mini-element (Arnold *et al.* 1984). This analysis leads to a consistent variational framework for the stabilized nodally integrated tetrahedral elements (Puso and Solberg 2006). Another pressure averaging approach (Guo *et al.* 2000, Hauret *et al.* 2007) based on macroelement technique (Stenberg 1990) also has been developed for near-incompressible elasticity problems leading to the uniform convergence in the nearly incompressible case.

Alternatively, several non-traditional numerical methods such as meshfree methods (Belytschko *et al.* 1994, Liu *et al.* 1995) and generalized finite element methods (Babuska and Melenk 1997, Duarte and Oden 1996) have been proposed to solve the incompressible locking problem. A pseudo-divergence-free interpolation for Element-free Galerkin method (Belytschko *et al.* 1994) was proposed (Vidal *et al.* 2003) to diffuse the divergence-free constraint which can be imposed a priori in a displacement-based Galerkin meshfree formulation. Another locking-free displacement-based Galerkin meshfree formulation which is an extension of finite element projection method (Chen *et al.* 1996) was presented (Chen *et al.* 2000) for the nonlinear analysis of rubber-like materials. Subsequently, various meshfree approaches have also been developed to alleviate the incompressible locking (De and Bathe 2001, Dolbow and Belytschko 1999, Ortiz *et al.* 2010) in the framework of B-bar or mixed formulations. Dolbow and Devan (2004) presented a geometrically nonlinear assumed strain method for the nonlinear analysis of hyperelastic materials involving displacement discontinuity where the strain is enriched based on the generalized finite element approach. Similar idea of using generalized finite element approach was presented (Srinivasan *et al.* 2008) in the framework of mixed finite element method for nonlinear analysis of near-incompressible rubber compounds. Recently, the iso-geometric discretization based on Non-Uniform Rational B-Splines (NURBS) (Hughes *et al.* 2005) has presented a promising alternative to solve the incompressible or near-incompressible problems. The high continuity of the NURBS interpolation allows us to solve the incompressible elasticity as an elliptic fourth-order problem in terms of a scalar stream function whose curl gives the displacement field (Auricchio *et al.* 2007). A nonlinear F-bar projection method (Elguedj *et al.* 2008) using the higher-order NURBS interpolation was also proposed for the nonlinear analysis of near-incompressible elasticity. Recently, a meshfree-enriched finite element method (ME-FEM) was proposed (Wu and Hu 2011) to overcome the incompressible locking problem. The meshfree-enriched linear element

is established by introducing a first-order convex meshfree approximation (Park *et al.* 2011, Wu and Koishi 2009, Wu *et al.* 2011) into a linear element with an enriched meshfree node. Additional strain smoothing procedure (Wu and Hu 2011) is developed in corporation with the meshfree-enriched finite element interpolation to acquire the discrete divergence-free property for the locking-free analysis. An equivalent mixed formulation was also derived in (Wu and Hu 2011) for the stability study of triangular and tetrahedral elements. Their numerical inf-sup (Bathe 1996) study indicates the pair of spaces in displacement and pressure fields is inf-sup stable. More recently, the ME-FEM has been extended for the study of large deformation problem in path-independent elastomers (Hu *et al.* 2012). Same strain smoothing technique was also applied to the linear finite elements leading to a two - level mesh re-partitioning scheme (Wu and Hu 2012) for the near-incompressible analysis.

The purpose of this paper is to present a nonlinear version of the meshfree-enriched finite element formulation using triangular elements and tetrahedron elements for general nonlinear metal forming analysis in path-dependent materials including contact. The reminder of the paper is outlined as follows: In the next Section, we provide an overview on the meshfree-enriched triangular element. In addition, a smoothing procedure on deformation gradients is introduced. In Section 3, we present a Lagrangian formulation of the meshfree-enriched finite element method for the nonlinear quasi-static and explicit dynamic analysis. A modified variational formulation is described and the discrete equation is derived. Mortar contact algorithm is also implemented to impose normal and tangential contact constraints. Two numerical examples are presented in Section 4 to demonstrate the accuracy and robustness of the proposed method. Final remarks are given in Section 5.

2. Experimental

2.1 Meshfree-enriched finite element triangular elements

This Section provides an overview on the construction of meshfree-enriched finite element interpolations in triangular elements. Same element construction technique was applied to tetrahedron elements leading to a linear 3D formulation which can be found in (Wu and Hu 2011) and thus is omitted in this paper. Let's consider a locally quasi-uniform triangulation M_h of the polygonal domain Ω , where M_h consists of simplexes and is denoted by $M_h = \cup_e T_e$. Each simplex or triangle T_e contains three corner nodes \mathbf{x}_I , $1 \leq I \leq 3$ and one enriched meshfree node \mathbf{x}_4 . Let $\mathbf{F}_e \in \mathbf{P}_1(\bar{T}_e)$ be the affine transformation that maps the reference triangle \bar{T}_e onto to the triangle $T_e \in M_h$ as depicted in Fig. 1 and defined by

$$\mathbf{F}_e : \bar{T}_e \rightarrow T_e, \mathbf{x} = \mathbf{F}_e(\boldsymbol{\xi}) = (F_e^1, F_e^2) = \left(\sum_{I=1}^3 x_I \Psi_I(\boldsymbol{\xi}, \eta), \sum_{I=1}^3 y_I \Psi_I(\boldsymbol{\xi}, \eta) \right) \quad \forall \boldsymbol{\xi} \in \bar{T}_e \quad (1)$$

where $\mathbf{x} = [x, y]^T$, $\boldsymbol{\xi} = [\xi, \eta]^T$ and $\mathbf{P}_1(\bar{T}_e) = span\{\Psi_I, I = 1, \dots, 4\}$ denotes the space contains a set of basis functions in \bar{T}_e .

In Fig. 1 the reference element \bar{T}_e is an equilateral triangle, with dark circles denoting the finite element node and open circles denoting the enriched meshfree node. The location of the enriched meshfree node in reference element \bar{T}_e is given by

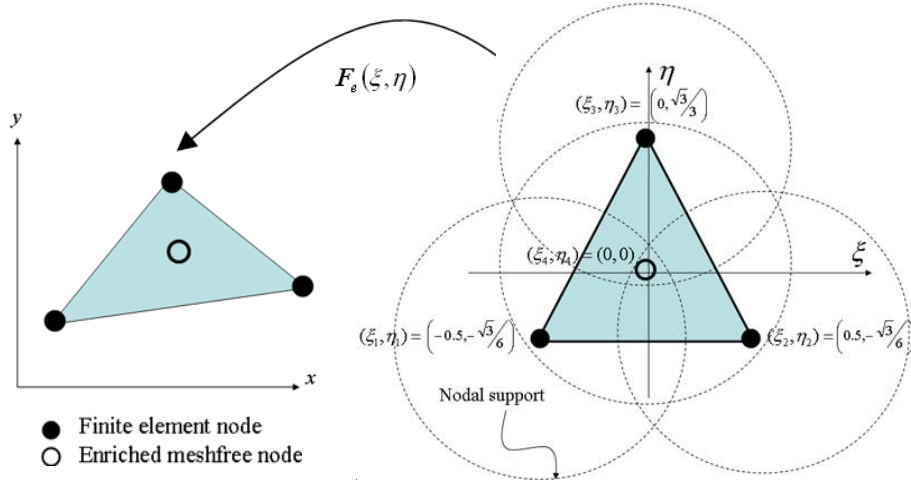


Fig. 1 Isoparametric mapping in the 4-noded meshfree-enriched triangular finite element

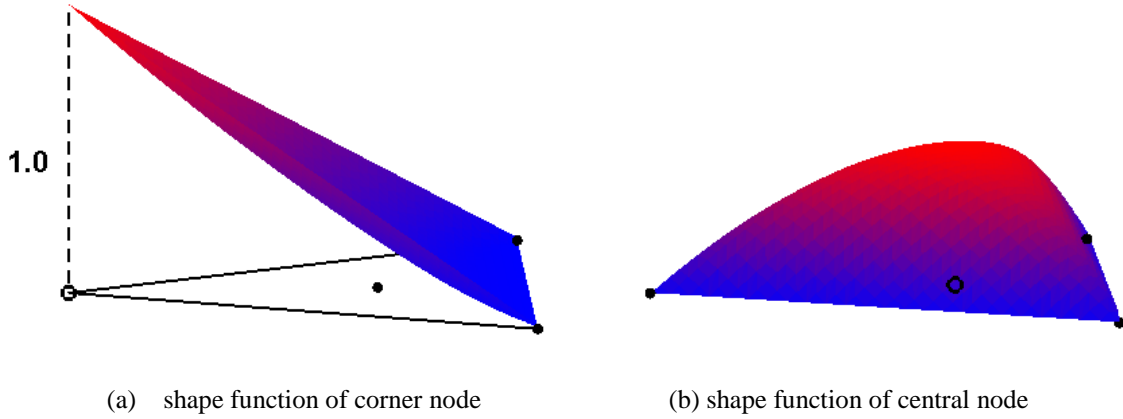
$$(\xi_4, \eta_4) = \left(\sum_{I=1}^3 \xi_I / 3, \sum_{I=1}^3 \eta_I / 3 \right) \quad (2)$$

which is the centroid of the reference element. $\xi_I = (\xi_I, \eta_I)$, $I = 1, 2, 3, 4$ are nodal co-ordinates of the reference element. The shape functions Ψ_I , $I = 1, 2, 3, 4$ of the reference element are constructed using a meshfree convex approximation. In this study, we employ the Generalized Meshfree Approximation (GMF) method (Wu *et al.* 2011) to obtain the meshfree convex approximation. The convex GMF approximation constructed using the inverse tangent basis function is denoted by GMF(*atan*). The cubic spline window function is chosen to be the weight function in GMF method. In this study, each node in Fig. 1 is assigned to a weight function with same circular support in the reference element \bar{T}_e . The element mapping in the meshfree-enriched finite element method has been proven (Wu and Hu 2011) to be bijective. In other words, the determinant of the Jacobian matrix computed using Eq. (1) in the element mapping is positive everywhere in the element. A detail derivation of GMF method and the corresponding mathematical properties can be found in (Wu *et al.* 2011).

Giving the four-noded ME-FEM shape functions, we define the following approximation space for the displacement field

$$\mathbf{V}^h(\Omega) = \left\{ \mathbf{v}^h : \mathbf{v}^h \in \mathbf{H}_0^1(\Omega), \mathbf{v}^h|_{T_e} = \bar{\mathbf{v}}^h \circ \mathbf{F}_e^{-1}, \bar{\mathbf{v}}^h \in \mathbf{P}_1(\bar{T}_e) \quad \forall T_e \in M_h \right\} \quad (3)$$

which consists of functions in Sobolev space $\mathbf{H}^1(\Omega)$ vanish on the boundary. Since the shape functions constructed using the GMF method are convex, they exhibit the following convexity properties which are not mutually $(\cdot, \cdot)_{\mathbf{V}^h}$ -orthonormal



(a) shape function of corner node (b) shape function of central node
 Fig. 2 GMF(atan) convex approximation in a 4-noded meshfree-enriched finite element

$$\begin{aligned}
 \Psi_I(\xi_J) &= \delta_{IJ} \quad 1 \leq I, J \leq 3 \\
 \Psi_4(\xi) &> 0 \quad \forall \xi \in \bar{T}_e \\
 \Psi_4(\xi) &= 0 \quad \forall \xi \in \partial\bar{T}_e \\
 \Psi_I(\xi_4) &> 0 \quad 1 \leq I \leq 3 \quad \text{and} \quad \Psi_4(\xi_4) \neq 1
 \end{aligned} \tag{4}$$

Fig. 2 shows the shape functions of a four-noded ME-FEM element using GMF(atan) approximation where the Kronecker-delta property is satisfied at the boundary (Wu *et al.* 2011). The shape functions of the ME-FEM element reduce to the standard linear finite element shape functions along the element edge that exhibit the convex approximation property.

2.2 Smoothing of deformation gradient in meshfree-enriched finite element triangular elements

In order to provide a locking-free analysis for the elastomers using meshfree-enriched triangular elements, an area-weighted strain smoothing scheme originally introduced (Wu and Hu 2011) in the near-incompressible linear elastic problem is adopted in this study for the smoothing of deformation gradient for the nonlinear hyperelastic problem. The strain smoothing technique was firstly proposed (Chen *et al.* 2001) and has been widely used in meshfree methods to enforce the linear exactness in Galerkin approach as well as to improve the computational efficiency. The strain smoothing technique in meshfree methods was also applied to finite element method providing a softening effect to improve the solution accuracy and led to various node-based, element-based and edge-based smoothed finite element formulations (Chen *et al.* 2010, He *et al.* 2009, Liu and Nguyen-Thoi 2010). The deformation gradient smoothing scheme is described in the following:

Let \mathbf{x}_I^J , $1 \leq I \leq 3$ be the three vertices of a triangular element $T_J \in M_h$. \mathbf{x}_4^J is the centroid of the triangular element T_J . We connect \mathbf{x}_4^J to the three vertices of the triangle by straight lines to divide the triangle into three sub-triangles S_l , S_m and S_n as shown in Fig. 3 Each sub

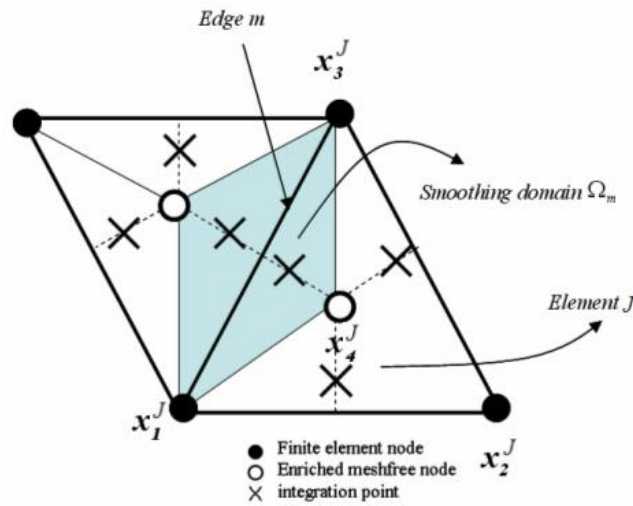


Fig. 3 Strain smoothing in ME-FEM triangle elements

-triangle S_m shares the element edge m of the triangle and carries one integration point. Since each sub-triangle occupies the same area, all three integration points are assigned to the same weight for the numerical integration. The location of the integration points ξ_{gk} , $1 \leq k \leq 3$ is chosen to form a symmetric pattern in the reference co-ordinate system such that for the enriched meshfree node I , one has

$$\sum_{k=1}^3 \frac{\partial \Psi_I(\xi_{gk})}{\partial \zeta} = 0 \tag{5}$$

and

$$\sum_{k=1}^3 \frac{\partial \Psi_I(\xi_{gk})}{\partial \eta} = 0 \tag{6}$$

By doing that, the integration point of each sub-triangle can be chosen to any point locating on the extension of the straight line associated with that sub-triangle as illustrated by the dashed line in Fig. 3. For simplicity, we choose the integration point to locate at the end of the extension line which is the midpoint of the element edge in this study. An eigenvalue analysis verifies that the proposed ME-FEM triangular element with this three-point integration rule does not contain spurious zero energy modes. The smoothing domain Ω_m corresponding to the edge m for the adjacent elements is defined as $\Omega_m = \cup_{S \in S_m} S$ and the smoothed deformation gradient is given in terms of its components by

$$\bar{F}_{ij}(X_{gk}) = \frac{1}{A_m} \int_{\Omega_m} F_{ij}(X_{gk}) \Phi_m(X) d\Omega \tag{7}$$

where A_m is the area of the smoothing domain Ω_m , $X_{gk}, k=1,2,3$ is the integration point of the element T_J that corresponds to the ξ_{gk} of \bar{T}_J . u_i^h is the approximation of displacement \mathbf{u} in i -component and is obtained by the linear combination of Lagrangian shape function of meshfree-enriched triangular element. It can be expressed by

$$u_i^h(\mathbf{X}) = \sum_{l=1}^4 \Psi_l(\mathbf{X}) u_{il}, \quad i=1,2 \quad (8)$$

where u_{il} is the nodal coefficient needs to be determined. $\Phi_m(\mathbf{x})$ in Eq. (7) is the characteristic or smoothing function of the smoothing domain Ω_m defined by

$$\Phi_m(\mathbf{X}) = \begin{cases} 1, & \text{if } \mathbf{X} \in \Omega_m \\ 0, & \text{else} \end{cases} \quad (9)$$

Subsequently, Eq. (7) can be rewritten using Eq. (8) to yield

$$\begin{aligned} \bar{F}_{ij}^h &= \frac{1}{A_m} \int_{\Omega_m} \left(\frac{\partial u_i^h}{\partial X_j} + \delta_{ij} \right) \Phi_m(\mathbf{X}) d\Omega = \frac{1}{A_m} \int_{\Omega_m} \left(\frac{\partial u_i^h}{\partial X_j} \right) \Phi_m(\mathbf{X}) d\Omega + \delta_{ij} \\ &= \frac{1}{A_m} \int_{\Omega_m} \sum_{l=1}^4 \left(\frac{\partial \Psi_l}{\partial X_j} u_{il} \right) \Phi_m(\mathbf{X}) d\Omega + \delta_{ij} \equiv \bar{\varphi}_{ij}^h + \delta_{ij} \end{aligned} \quad (10)$$

where

$$\bar{\varphi}_{ij}^h = \frac{1}{A_m} \int_{\Omega_m} \sum_{l=1}^4 \left(\frac{\partial \Psi_l}{\partial X_j} u_{il} \right) \Phi_m(\mathbf{X}) d\Omega \quad (11)$$

Since the smoothed deformation gradient is defined locally on each smoothing domain Ω_m and no continuity conditions are applied to the boundaries of Ω_m , the approximation space of smoothed deformation gradient can be defined by

$$\bar{\mathbf{E}}^h(\Omega) = \left\{ \bar{\mathbf{F}}^h : \bar{\mathbf{F}}^h \in L^2(\Omega), \bar{\mathbf{F}}^h \text{ contains piecewise constants } \forall \Omega_m \in \mathcal{M}_h \right\} \quad (12)$$

In linear elastic problem, an assumed strain method (Simo and Hughes 1986) can be employed to formulate the discrete equations (Wu and Hu 2011) where pressure is calculated via post-processing from the following constitutive relation

$$p^h = -\lambda \overline{\text{div}(\mathbf{u}^h)} = -\lambda \text{tr } \bar{\boldsymbol{\varepsilon}}(\mathbf{u}^h) = -\lambda \frac{1}{A_m} \int_{\Omega_m} \text{tr} [\boldsymbol{\varepsilon}(\mathbf{u}^h)] \Phi_m(\mathbf{X}) d\Omega \quad (13)$$

The symbol λ is the Lamé constant or bulk modulus which is related to the Young's modulus E and Poisson ratio ν by $\lambda = (\nu E) / (1 + \nu)(1 - 2\nu)$.

Although the pressure does not directly involve in the computation, the well-posedness of the

problem in near-incompressible regime is still subject to a stability condition between the displacement space \mathbf{V}^h and an implicit pressure space \mathbf{P}^h induced by Eq. (13). Alternatively, an equivalent mixed formulation was derived (Wu and Hu 2011) for the stability study of meshfree-enriched finite element method in the near-incompressible limit. Their numerical inf-sup results indicate the pair of spaces $(\mathbf{V}^h, \mathbf{P}^h)$ is inf-sup stable.

3. Nonlinear ME-FEM formulation for large deformation analysis

Consider the following equation of motion with boundary and initial conditions

$$\rho \ddot{u}_i = \sigma_{ij,j} + b_i \quad \text{in } \Omega \quad (14)$$

$$\sigma_{ij} n_j = h_i \quad \text{on } \Gamma^h \quad (15)$$

$$u_i = d_i \quad \text{on } \Gamma^d \quad (16)$$

$$u_i(\mathbf{X}, 0) = u_i^0(\mathbf{X}) \quad (17)$$

$$v_i(\mathbf{X}, 0) = v_i^0(\mathbf{X})$$

where ρ is material density, n_i is the surface normal in the deformed configuration, u_i^0 and v_i^0 is the initial displacement and velocity. The variational equation is formulated to find $u_i(\mathbf{X}, t) \in H_d^1$, such that for all $\delta u_i \in H_0^1$, the following equation is satisfied

$$\delta U = \int_{\Omega} \delta u_i \rho \ddot{u}_i d\Omega + \int_{\Omega} \delta u_{i,j} \sigma_{ij} d\Omega - \int_{\Omega} \delta u_i b_i d\Omega - \int_{\Gamma^h} \delta u_i h_i d\Gamma = 0 \quad (18)$$

with the initial condition (17)

3.1 Modified variational functional and material nonlinearity in quasi-static analysis

For path-independent material, the energy function is established in the current configuration using the updated Lagrangian formulation. By introducing the Lagrangian strain smoothing, we can obtain the modified variational equation similar as in the assumed strain method

$$\delta U^h = \int_{\Omega} \delta \bar{u}_{i,j}^h \bar{\sigma}_{ij} d\Omega - \delta W_{ext} \quad (19)$$

where $\bar{\sigma}_{ij}$ is the smoothed Cauchy stress, $\bar{u}_{i,j}^h \equiv \overline{\partial u_i / \partial x_j}$ is the smoothed strain, \mathbf{x} is the spatial coordinate calculated from material coordinate \mathbf{X} and displacement $\mathbf{u}(\mathbf{X})$ and Ω represents the domain of the current configuration. The linearization of Eq. (19) is

$$\Delta \delta U^h = \int_{\Omega} \delta \bar{u}_{i,j}^h (\bar{C}_{ijkl}^{\sigma} + \bar{T}_{ijkl}^{\sigma}) \Delta \bar{u}_{k,l}^h d\Omega - \Delta \delta W_{ext} \quad (20)$$

where \bar{C}_{ijkl}^σ is the material response tensor and \bar{T}_{ijkl}^σ is geometric response tensor. Considering that the ME-FEM shape function and the smoothed gradient of displacement approximation are defined in the original configuration, we transform the variational Eqs. (19) and (20) to the undeformed configuration as

$$\delta U^h = \int_{\Omega_0} \overline{\frac{\partial \delta u_i^h}{\partial X_k}} \bar{F}_{kj}^{-1} \bar{\sigma}_{ij} J_0 d\Omega_0 - \delta W_{ext} \quad (21)$$

$$\Delta \delta U^h = \int_{\Omega_0} \overline{\frac{\partial \delta u_i^h}{\partial X_m}} \bar{F}_{mj}^{-1} (\bar{C}_{ijkl}^\sigma + \bar{T}_{ijkl}^\sigma) \bar{F}_{nl}^{-1} \overline{\frac{\partial \Delta u_k^h}{\partial X_n}} J_0 d\Omega_0 - \Delta \delta W_{ext} \quad (22)$$

where Ω_0 is undeformed domain, $J_0 = \det(\mathbf{F})$. \bar{F}_{ij} is the smoothed deformation gradient. In the computation, \bar{F}^{-1} in Eqs. (21) and (22) is calculated only at the integration points, which can be obtained by taking the direct inverse of \bar{F} point-wise.

The smoothed incremental strain $\Delta \bar{u}_{i,j}$ at the integration point \mathbf{X}_{gk} is computed by

$$\Delta \bar{u}_{i,j}(\mathbf{X}_{gk}) = \overline{\frac{\partial \Delta u_i}{\partial X_m}} \bar{F}_{mj}^{-1} = \Delta \bar{F}_{im}(\mathbf{X}_{gk}) \bar{F}_{mj}^{-1}(\mathbf{X}_{gk}) \quad (23)$$

where $\bar{F}_{im}(\mathbf{X}_{gk})$ is smoothed deformation gradient computed by Eq. (10). Subscribing Eqs. (10) and (23) into Eq. (22) leads to the following linearization of variational equation

$$\Delta \delta U^h = \int_{\Omega_0} \delta u_i^h \rho \Delta \bar{u}_i^h d\Omega_0 + \int_{\Omega_0} \delta \bar{\varphi}_{im}^h \bar{F}_{mj}^{-1} \left[\bar{C}_{ijkl}^\sigma(\bar{F}^h) + \bar{T}_{ijkl}^\sigma(\bar{F}^h) \right] \bar{F}_{nl}^{-1} \Delta \bar{\varphi}_{kn}^h \bar{J}_0(\bar{F}^h) d\Omega_0 - \Delta \delta W_{ext} \quad (24)$$

Introducing the approximations of displacement in Eq. (8) and smoothed deformation gradient in Eq. (10) into Eq. (24) yields the stiffness matrix and internal force vector

$$\bar{\mathbf{K}}_{IJ} = \int_{\Omega_0} \bar{\mathbf{B}}_I^T \bar{\mathbf{G}}^T \left[\bar{\mathbf{C}}^\sigma(\bar{\mathbf{F}}^h) + \bar{\mathbf{T}}^\sigma(\bar{\mathbf{F}}^h) \right] \bar{\mathbf{G}} \bar{\mathbf{B}}_J \bar{J}_0 d\Omega_0 \quad (25)$$

$$\mathbf{f}_I^{int} = \int_{\Omega_0} \bar{\mathbf{B}}_I^T \bar{\mathbf{G}}^T \bar{\boldsymbol{\sigma}}(\bar{\mathbf{F}}^h) \bar{J}_0 d\Omega_0 \quad (26)$$

where, in two-dimensional problem

$$\bar{\mathbf{G}} = \begin{bmatrix} \bar{F}_{11}^{-1} & 0 & \bar{F}_{21}^{-1} & 0 \\ 0 & \bar{F}_{22}^{-1} & 0 & \bar{F}_{12}^{-1} \\ \bar{F}_{12}^{-1} & \bar{F}_{21}^{-1} & \bar{F}_{22}^{-1} & \bar{F}_{11}^{-1} \end{bmatrix}, \quad \bar{\boldsymbol{\sigma}} = \begin{bmatrix} \bar{\sigma}_{11} \\ \bar{\sigma}_{22} \\ \bar{\sigma}_{12} \end{bmatrix} \quad (27)$$

and $\bar{\mathbf{B}}_I$ is the smoothed gradient matrix given by

$$\bar{\mathbf{B}}_l = \frac{1}{A_m} \begin{bmatrix} \int_{\Omega_m} \left(\frac{\partial \Psi_l}{\partial X_1} \right) \Phi_m(\mathbf{X}) d\Omega & 0 \\ 0 & \int_{\Omega_m} \left(\frac{\partial \Psi_l}{\partial X_2} \right) \Phi_m(\mathbf{X}) d\Omega \\ \int_{\Omega_m} \left(\frac{\partial \Psi_l}{\partial X_2} \right) \Phi_m(\mathbf{X}) d\Omega & 0 \\ 0 & \int_{\Omega_m} \left(\frac{\partial \Psi_l}{\partial X_1} \right) \Phi_m(\mathbf{X}) d\Omega \end{bmatrix} \quad (28)$$

3.2 Discrete formulation for explicit dynamic analysis with mortar contact algorithm

For explicit dynamic analysis of general metal forming problem involving contact, the modified variational Eq. (21) is extended as follows

$$\delta U^h = \int_{\Omega_0} \delta u_i^h \rho_0 \dot{u}_i^h d\Omega_0 + \int_{\Omega_0} \frac{\partial \delta u_i^h}{\partial X_k} \bar{F}_{kj}^{-1} \bar{\sigma}_{ij} J_0 d\Omega_0 - \delta W_{ext} - \delta W_c \quad (29)$$

where ρ_0 is the material density in the undeformed configuration and δW_c denotes the variational potential energy due to contact constraints. For simplicity, we consider one deformable body contacting with rigid counterparts in forming analysis so that δW_c can be expressed by

$$\delta W_c = \int_{\Gamma^c} \delta u_i^h t_i^c d\Gamma \quad (30)$$

where Γ^c is the contact surface of deformable body and t_i^c is contact traction. Introducing the ME-FEM approximation (8) and the smoothed deformation gradient (10) into (29) leads to the matrix form of explicit equation

$$\mathbf{M}\mathbf{a} = \mathbf{f}^{ext} + \mathbf{f}^c - \mathbf{f}^{int} \quad (31)$$

where \mathbf{a} is the nodal acceleration vector. The nodal lumped mass and force vectors are given as

$$\begin{aligned} m_l &= \int_{\Omega} \rho_0 \Psi_l d\Omega_0 \\ \mathbf{f}_l^{int} &= \int_{\Omega_0} \bar{\mathbf{B}}_l^T \bar{\mathbf{G}}^T \bar{\boldsymbol{\sigma}}(\bar{\mathbf{F}}^h) \bar{\mathbf{J}}_0 d\Omega_0 \\ \mathbf{f}_l^{ext} &= \int_{\Gamma^h} \mathbf{h} \Psi_l d\Gamma + \int_{\Omega} \mathbf{b} \Psi_l d\Omega \\ \mathbf{f}_l^c &= \int_{\Gamma^c} \mathbf{t}^c \Psi_l d\Gamma \end{aligned} \quad (32)$$

where, for tow-dimensional problem, $\bar{\mathbf{B}}_l$ and $\bar{\mathbf{G}}$ are defined in Eqs. (28) and (27),

respectively. The contact traction \mathbf{t}^c remains to be computed by imposing contact constraints through the mortar contact algorithm (Puso and Laursen 2004, Yang *et al.* 2005), which is briefly summarized as below.

Let \mathbf{u}^r denote the displacement of rigid master contact part. We start from two-body mortar contact virtual work defined on the non-mortar slave contact surface Γ^c

$$\int_{\Gamma^c} \boldsymbol{\lambda}^h \cdot (\delta \mathbf{u}^h - \delta \mathbf{u}^r) d\Gamma = 0 \quad (33)$$

where $\boldsymbol{\lambda}$ is the mortar multiplier representing the contact traction. The mortar contact interpolation is performed as follows

$$\begin{aligned} \boldsymbol{\lambda}^h(\mathbf{x}) &= \sum_{I=1}^{n_s} N_I(\mathbf{x}(\mathbf{X})) \boldsymbol{\lambda}_I \quad \mathbf{X} \in \Gamma^c \\ \mathbf{u}^h(\mathbf{x}) &= \sum_{I=1}^{n_s} N_I(\mathbf{x}(\mathbf{X})) \mathbf{u}_I \quad \mathbf{X} \in \Gamma^c \\ \mathbf{u}^r(\mathbf{x}^r) &= \sum_{I=1}^{n_m} N_I^r(\mathbf{x}^r(\mathbf{X}^r)) \mathbf{u}_I^r \quad \mathbf{X}^r \in \Gamma^{rc} \end{aligned} \quad (34)$$

where n_s and n_m are numbers of nodes on the slave and master surfaces, respectively; N_I and N_I^r are finite element interpolation functions defined on the current configuration of piece-wise contact segments of Γ^c and master contact surface Γ^{rc} , respectively. Substituting (34) into (33) leads to the following discrete form

$$\sum_{I=1}^{n_s} \boldsymbol{\lambda}_I \cdot \left[\sum_{J=1}^{n_s} w_{IJ} \delta \mathbf{u}_J - \sum_{J=1}^{n_m} w_{IJ}^r \delta \mathbf{u}_J^r \right] = 0 \quad (35)$$

where w_{IJ} and w_{IJ}^r are referred as mortar integrals:

$$\begin{aligned} w_{IJ} &= \int_{\Gamma^c} N_I(\mathbf{x}(\mathbf{X})) N_J(\mathbf{x}(\mathbf{X})) d\Gamma \\ w_{IJ}^r &= \int_{\Gamma^c} N_I(\mathbf{x}(\mathbf{X})) N_J^r(\tilde{\mathbf{x}}(\mathbf{X})) d\Gamma \end{aligned} \quad (36)$$

$\tilde{\mathbf{x}}(\mathbf{X})$ defines the closest point projection from slave contact point $\mathbf{x}(\mathbf{X})$ to master surface. In order to impose the normal and tangential contact constraints, the nodal mortar multiplier is decomposed by

$$\boldsymbol{\lambda}_I = \lambda_I^{Normal} \mathbf{n}_I + \boldsymbol{\lambda}_I^{Tangential} \quad (37)$$

where \mathbf{n}_I is unit averaged normal vector at slave node I . The definition of \mathbf{n}_I on a discretized contact surface can be found in the literature (Yang *et al.* 2005). Substituting (37) into (35) yields

$$\sum_{I=1}^{n_s} (\lambda_I^{Normal} \delta \chi_I + \lambda_I^{Tangential} \cdot \delta \mathbf{s}_I) = 0 \quad (38)$$

where, in three-dimensional problem, the mortar projected and slip gaps at slave node I are obtained as

$$\begin{aligned} \chi_I &= \mathbf{n}_I \cdot \kappa_A \left(\sum_{J=1}^{n_s} w_{IJ} \mathbf{x}_J - \sum_{J=1}^{n_m} w_{IJ}^r \mathbf{x}_J^r \right) \\ \mathbf{s}_I &= (\mathbf{I} - \mathbf{n}_I \otimes \mathbf{n}_I) \cdot \kappa_A \left(\sum_{J=1}^{n_s} w_{IJ} \mathbf{x}_J - \sum_{J=1}^{n_m} w_{IJ}^r \mathbf{x}_J^r \right) \end{aligned} \quad (39)$$

\mathbf{I} is unit tensor and κ_A is a normalization parameter. In mortar contact algorithm, the penalty regularization (Kikuchi and Oden 1988) of augmented Lagrangian scheme is often used to impose the contact constraints, which requires the computation of the incremental tangential slip gap (Puso and Laursen 2004)

$$\begin{aligned} \Delta \mathbf{s}_I &= (\mathbf{I} - \mathbf{n}_I \otimes \mathbf{n}_I) \cdot \kappa_A \left\{ \sum_{J=1}^{n_s} [w_{IJ,k+1} - w_{IJ,k}] \mathbf{x}_{J,k} \right. \\ &\quad \left. - \sum_{J=1}^{n_m} [w_{IJ,k+1}^r - w_{IJ,k}^r] \mathbf{x}_{J,k}^r - \chi_{A,k} \mathbf{n}_A \right\} \end{aligned} \quad (40)$$

where subscripts k and $k+1$ indicate the k -th and $(k+1)$ th time steps, respectively. Note that (40) is an invariant form in rigid body rotation. The mortar contact normal pressure λ_A^{Normal} is subject to Kuhn-Tucker conditions

$$\lambda_A^{Normal} \geq 0, \chi_A \leq 0, \lambda_A^{Normal} \chi_A = 0 \quad (41)$$

Imposing (41) by penalty regularization leads to the following contact pressure

$$\lambda_I^{Normal} = \begin{cases} -\alpha^{Normal} \chi_I & \chi_I \leq 0 \\ 0 & \text{otherwise} \end{cases} \quad (42)$$

where α^{Normal} is normal penalty parameter. In the tangential contact direction, we first assume no slip from the k -th time step to the $(k+1)$ th and trial frictional traction can be expressed by

$$\left(\lambda_I^{Tangential} \right)_{k+1}^{trial} = \left(\lambda_I^{Tangential} \right)_k + \alpha^{Tangential} \Delta \mathbf{s}_I \quad (43)$$

where $\alpha^{Tangential}$ is frictional penalty parameter. The frictional contact traction is then corrected

based on the slip condition. If the Coulomb frictional contact model is used, the corrected frictional contact traction at the $(k+1)$ th time step is given by

$$\left(\lambda_I^{Tangential}\right)_{k+1}^{corrected} = \begin{cases} \left(\lambda_I^{Tangential}\right)_{k+1}^{trial} & \left\| \left(\lambda_I^{Tangential}\right)_{k+1}^{trial} \right\| \leq \mu \lambda_I^{Normal} \\ \mu \lambda_I^{Normal} \frac{\left(\lambda_I^{Tangential}\right)_{k+1}^{trial}}{\left\| \left(\lambda_I^{Tangential}\right)_{k+1}^{trial} \right\|} & \left\| \left(\lambda_I^{Tangential}\right)_{k+1}^{trial} \right\| > \mu \lambda_I^{Normal} \end{cases} \quad (44)$$

where μ is Coulomb frictional parameter.

4. Numerical examples

In this Section, the nonlinear performance of the meshfree-enriched triangular and tetrahedron elements with area-weighted strain smoothing (ME-Tri-AW) is evaluated in two examples: (1) two-dimensional punch problem using triangular elements in quasi-static analysis; (2) three-dimensional forming problem using tetrahedron elements in explicit dynamic analysis. In constructing the ME-FEM approximation, the GMF kernel is chosen to be the cubic B-spline function. Since the Kronecker-delta property of ME-FEM shape functions is preserved, no special essential boundary condition and contact condition treatments are required in the computation. A standard Newton-Raphson method is employed to solve the nonlinear equation in quasi-static analysis.

4.1 Punch problem

The punch example considers an elaso-plastic material subjected to displacement-controlled rigid footing under highly constrained boundaries as shown in Fig. 4. The contact between the rigid tool and workpiece is assumed to be frictionless. The material properties are: Young's modulus $E = 2.0\text{GPa}$, Poisson's ratio $\nu = 0.3$ and an isotropic hardening rule is given by

$$\sigma_y(\bar{e}^p) = \sigma_y^0 \left(1 + \alpha \bar{e}^p\right)^\beta \quad (45)$$

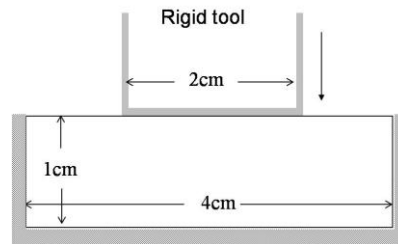


Fig. 4 Strain smoothing in ME-FEM triangle elements

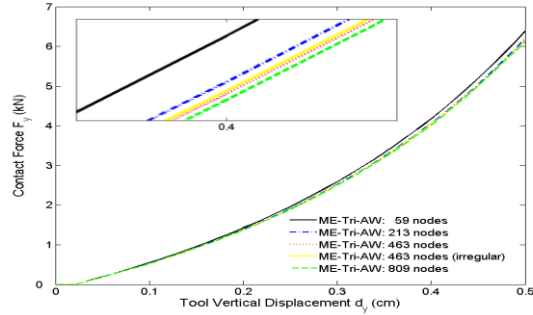
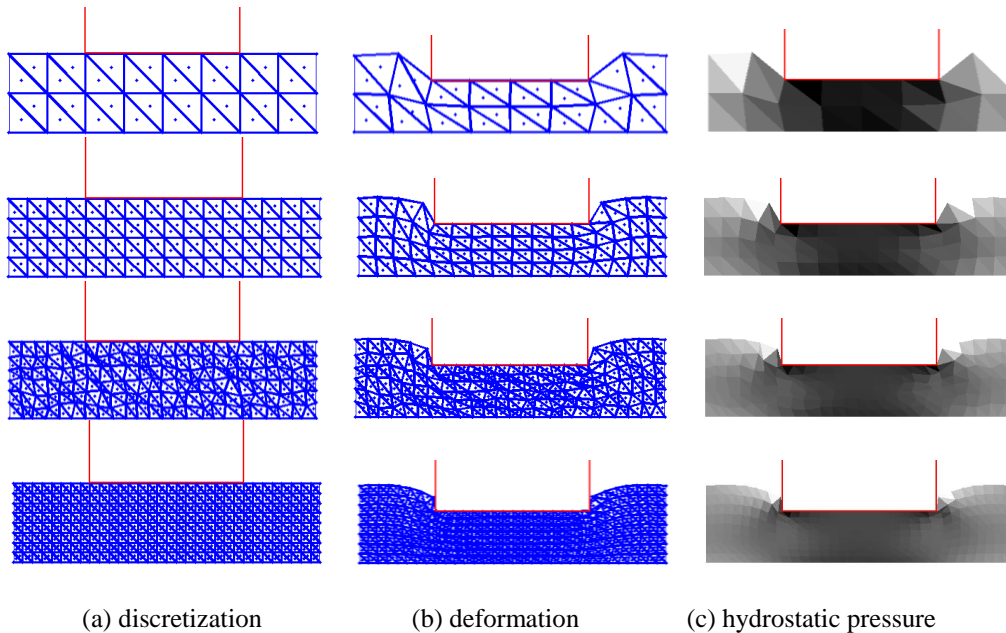


Fig. 5 Strain smoothing in ME-FEM triangle elements



(a) discretization (b) deformation (c) hydrostatic pressure

Fig. 6 ME-Tri-AW results using four different discretizations ($d_y = 0.35\text{cm}$)

where σ_y is yield radius and \bar{e}^p is effective plastic strain, respectively and $\sigma_y^0 = 0.02\text{GPa}$, $\alpha = 1.0\text{GPa}$, $\beta = 1.1$.

The load-displacement responses from ME-Tri-AW using five different mesh refinements are shown in Fig. 5. These results depict the convergence of ME-Tri-AW as the mesh is refined. Fig. 6 shows the deformation and pressure contour of ME-Tri-AW results when the rigid tool reaches vertical displacement of $d_y = 0.35\text{cm}$. As we can see, ME-Tri-AW achieves desirable deformation and smooth pressure results. The convergence study in Fig. 5 also indicates that the ME-Tri-AW solutions are insensitive to the mesh irregularity.

4.2 Sphere compression analysis

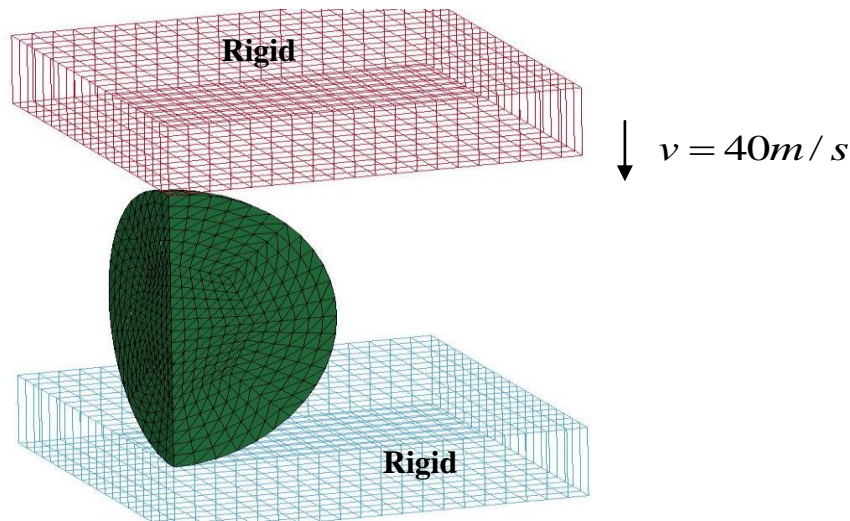


Fig. 7 Description of sphere compression problem

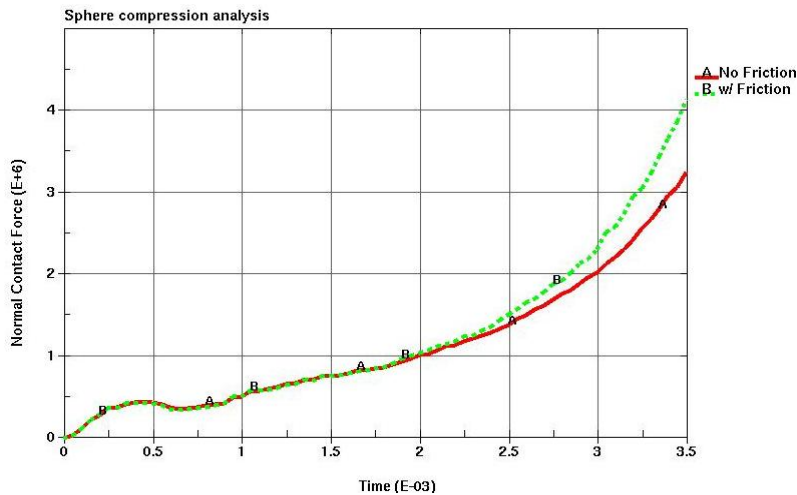


Fig. 8 Normal contact force comparison

This sphere compression test is conducted using a quarter model with symmetric boundary conditions, as shown in Fig. 7. The undeformed sphere radius is 0.1m. The material properties are: Density $\rho = 2750\text{kg/m}^3$, Young's modulus $E = 70.0\text{GPa}$, Poisson's ratio $\nu = 0.3$ and an isotropic hardening rule with $\sigma_y^0 = 0.1\text{GPa}$, $\alpha = 0.1\text{GPa}$, $\beta = 1.0$. The discretization has 19,562 ME-FEM elements. Two analyses are performed using frictionless contact model and Coulomb frictional contact model ($\mu = 0.2$), respectively.

Fig. 8 compares the normal contact force results from two analyses. Both results match very well in the initial stage where the contact surface is limited. As expected, the frictional contact model is more constrained and results in large normal contact force as compression operation proceeds. No oscillated contact forces are observed in both analyses.

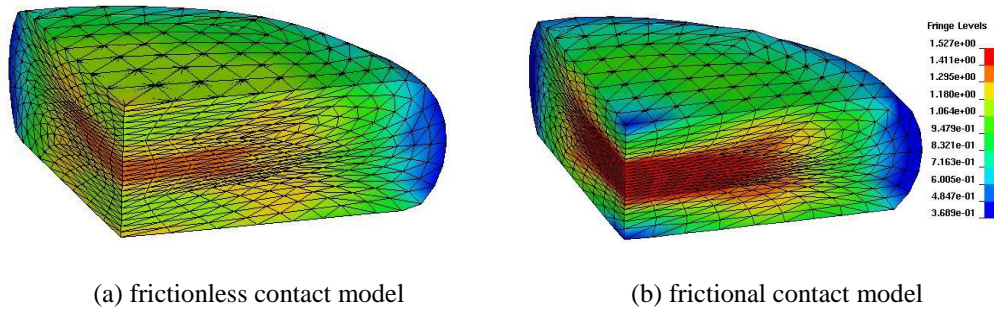


Fig. 9 Effective plastic strain contour at

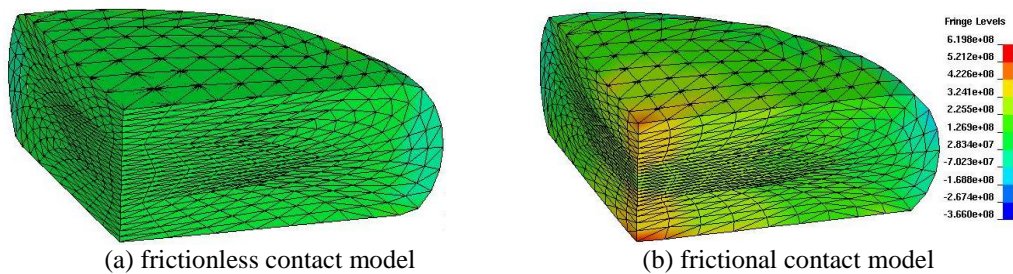


Fig. 10 Pressure contour at

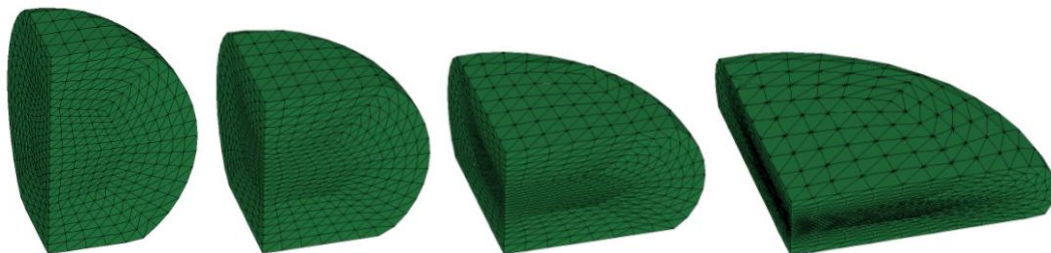


Fig. 11 Progressive deformations of sphere compression with frictional contact

The effective plastic strain and pressure contours are compared in Fig. 9 and Fig. 10 respectively. The frictional solution shows a higher effective plastic strain level subjected to the frictional contact constraint. The higher effective plastic strain result yields to a larger contact force as reported in Fig. 8. Both frictionless and frictional solutions are free of pressure oscillation as shown in Fig. 10. Fig. 11 shows the sphere progressive deformations of the frictional contact model. As we can see, ME-FEM generates smooth results even in very severe deformation. There is no unstable deformation mode observed in the ME-FEM solution.

5. Conclusions

A nonlinear formulation of meshfree-enriched finite element method (ME-FEM) is presented

for metal forming analysis. We start with an introduction of smoothed deformation gradients constructed using a convex meshfree approximation (Wu *et al.* 2011) based on a meshfree-enriched finite element triangulation proposed in Wu and Hu (2011). The introduced smoothed deformation gradient allows us to degenerate the three-fields Hu-Washizu-de Veubeke variational formulation to a displacement-based modified variational formulation that can be solved with relatively ease in the nonlinear analysis. As an advanced and robust contact algorithm, the mortar method is implemented in the explicit nonlinear formulation for dynamic analysis. The presented nonlinear formulation has demonstrated its accuracy and robustness through benchmark examples and proven it is free of volumetric locking and free of pressure oscillation for the path-dependent materials involving contact. In summary, the proposed nonlinear meshfree-enriched finite element formulation offers the following main attractions for the large deformation analysis in path-dependent materials: (1) its simplicity to be fitted into the conventional displacement-based finite element code and solved by the standard direct solver; (2) its convenience in enriching the meshfree nodes without redefining the boundary and contact conditions; (3) its accuracy and robustness in delivering volumetric locking-free and pressure oscillation-free solution in nonlinear finite strain analysis.

Acknowledgements

The authors would like to thank Dr. John O. Hallquist of LSTC for his support to this research.

References

- Andrade Pires, F.M., de Souza Neto, E.A. and de la Cuesta Padilla, J.L. (2004), "An assessment of the average nodal volume formulation for the analysis of nearly incompressible solids under finite strains", *Int. J. Numer. Meth. Eng.*, **20**, 569-583.
- Arnold, D.N., Brezzi, F. and Franca, L.P. (1984), "A stable finite element for the Stokes equations", *Calcolo*, **21**, 337-344.
- Auricchio, F., Beirão de Veiga, L., Buffam, C., Lovadina, A., Reali, A. and Sangalli, G. (2007), "A fully locking-free isogeometric approach for plane linear elasticity problems: a stream function formulation", *Comput. Meth. Appl. Mech. Eng.*, **197**, 160-172.
- Bathe, K.J. (1996), *Finite element procedures*, Prentice-Hall, New Jersey.
- Babuska, I. (1973), "The finite element method with Lagrangian multipliers", *Numer. Math.*, **20**, 179-192.
- Babuska, I. and Melenk, J.M. (1997), "The partition of unity method", *Int. J. Numer. Methods Eng.*, **40**, 727-758.
- Belytschko, T., Lu, Y.Y. and Gu, L. (1994), "Element-free Galerkin methods", *Int. J. Numer. Meth. Eng.*, **37**, 229-256.
- Belytschko, T., Liu, W.K. and Moran, B. (2001), *Nonlinear finite elements for continua and structures*, (Third Ed.), John Wiley & Sons, New York.
- Bonet, J. and Burton, A.J. (1998), "A simple average nodal pressure tetrahedral element for incompressible and nearly incompressible dynamic explicit applications", *Commun. Numer. Meth. Eng.*, **14**, 437-449.
- Chen, L., Liu, G.R., Nourbakhsh-Nia, N. and Zeng, K. (2010), "A singular edge-based smoothed finite element method (ES-FEM) for biomaterial interface cracks", *Comput. Mech.*, **45**, 109-125.
- Chen, J.S., Pan, C. and Wu, C.T. (1996), "A pressure projection method for nearly incompressible rubber hyperelasticity, Part I: Theory", *J. Appl. Mech.*, **63**, 862-868.
- Chen, J.S., Wu, C.T. and Pan, C. (1996), "A pressure projection method for nearly incompressible rubber

- hyperelasticity, Part II: Applications”, *J. Appl. Mech.*, **63**, 869-876.
- Chen, J.S., Han, W., Wu, C.T. and Duan, W. (1997), “On the perturbed Lagrangian formulation for nearly incompressible and incompressible hyperelasticity”, *Comput. Meth. Appl. Mech. Eng.*, **142**, 335-351.
- Chen, J.S., Yoon, S., Wang, H.P. and Liu, W.K. (2000), “An improved reproducing kernel particle method for nearly incompressible finite elasticity”, *Comput. Meth. Appl. Mech. Eng.*, **181**, 117-145.
- Chen, J.S., Wu, C.T., Yoon, S. and You, Y. (2001), “A stabilized conforming nodal integration for Galerkin mesh-free methods”, *Int. J. Numer. Meth. Eng.*, **50**, 435-466.
- De, S. and Bathe, K.J. (2001), “Displacement/pressure mixed interpolation in the method of finite spheres”, *Int. J. Numer. Meth. Eng.*, **51**, 275-292.
- Dolbow, J. and Belytschko, T. (1999), “Volumetric locking in the element free Galerkin method”, *Int. J. Numer. Meth. Eng.*, **46**, 925-942.
- Dolbow, J. and Devan, A. (2004), “Enrichment of enhanced assumed strain approximations for representing strong discontinuities patch test”, *Int. J. Numer. Meth. Eng.*, **59**, 47-67.
- Duarte, C.A. and Oden, J.T. (1996), “An h-p adaptive method using clouds”, *Comput. Meth. Appl. Mech. Eng.*, **39**, 237-262.
- Elguedj, T., Bazilevs, Y., Calo, V.M. and Hughes, T.J.R. (2008), “ \bar{B} and \bar{F} projection methods for nearly incompressible linear and non-linear elasticity and plasticity using higher-order NURBS elements”, *Comput. Meth. Appl. Mech. Eng.*, **197**, 2732-2762.
- Guo, Y., Ortiz, M., Belytschko, T. and Repetto, E.A. (2000), “Triangular composite finite elements”, *Comput. Meth. Appl. Mech. Eng.*, **47**, 287-316.
- Hauret, P., Kuhl, E. and Ortiz, M. (2007), “Diamond elements: a finite element/discrete-mechanics approximation scheme with guaranteed optimal convergence in incompressible elasticity”, *Comput. Meth. Appl. Mech. Eng.*, **72**, 253-294.
- He, Z.C., Liu, G.R., Zhong, Z.H., Wu, S.C., Zhang, G.Y. and Cheng, A.G. (2009), “An edge-based smoothed finite element method (ES-FEM) for analyzing three-dimensional acoustic problems”, *Comput. Meth. Appl. Mech. Eng.*, **199**, 20-33.
- Hu, W., Wu, C.T. and Koishi, M. (2012), “A displacement-based nonlinear finite element formulation using meshfree-enriched triangular elements for the two-dimensional large deformation analysis of elastomers”, *Finite Elem. Anal. Des.*, **50**, 161-172.
- Hughes, T.J.R. (2000), *The finite element method*, Prentice-Hall: Englewood Cliffs, NJ.
- Hughes, T.J.R., Cottrell, J.A. and Bazilevs, Y. (2005), “Isogeometric analysis: CAD, finite elements, NURBS, exact geometry and mesh refinement”, *Comput. Meth. Appl. Mech. Eng.*, **194**, 4135-4195.
- Kikuchi, N. and Oden, J.T. (1988), *Contact Problems in Elasticity: A Study of Variational Inequalities and Finite Element Methods*, SIAM, Philadelphia.
- Krysl, P. and Zhu, B. (2008), “Locking-free continuum displacement finite elements with nodal integration”, *Comput. Meth. Appl. Mech. Eng.*, **76**, 1020-1043.
- Lamichhane, B.P. (2009), “Inf-sup stable finite element pairs based on dual meshes and bases for nearly incompressible elasticity”, *IMA J. Numer. Anal.*, **29**, 404-420.
- Liu, G.R. and Nguyen-Thoi, T. (2010), *Smoothed finite element method*, CRC Press, Boca Raton.
- Liu, W.K., Ong, J.S.J. and Uras, R.A. (1986), “Finite element stabilization matrices-a unification approach”, *Comput. Meth. Appl. Mech. Eng.*, **53**, 13-46.
- Liu, W.K., Jun, S., Li, S., Adee, J. and Belytschko, T. (1995), “Reproducing kernel particle methods for structural dynamics”, *Comput. Meth. Appl. Mech. Eng.*, **38**, 1655-1679.
- Malkus, D.S. and Hughes, T.J.R. (1978), “Mixed finite element methods-reduced and selective integration techniques: a unification of concepts”, *Comput. Meth. Appl. Mech. Eng.*, **15**, 63-81.
- Ortiz, A., Puso, M.A. and Sukumar, N. (2010), “Maximum-Entropy meshfree method for compressible and near-incompressible elasticity”, *Comput. Meth. Appl. Mech. Eng.*, **199**, 1859-1871.
- Park, C.K., Wu, C.T. and Kan, C.D. (2011), “On the analysis of dispersion property and stable time step in meshfree method using the generalized meshfree approximation”, *Finite Elem. Anal. Des.*, **47**, 683-697.
- Peen, R.W. (1970), “Volume changes accompanying the extension of rubber”, *Trans. Soc. Rheol.*, **14**, 509-517.

- Puso, M.A. and Laursen, T.A. (2004), "A mortar segment-to-segment contact method for large deformation solid mechanics", *Comput. Meth. Appl. Mech. Eng.*, **193**, 601-629.
- Puso, M.A. and Solberg, J. (2006), "A stabilized nodally integrated tetrahedral", *Comput. Meth. Appl. Mech. Eng.*, **67**, 841-867.
- Rivlin, R.S. (1949), "Large elastic deformation of isotropic materials, Part VI, further results in the theory of torsion, shear and flexure", *Philos. Trans. R. Soc. of London*, A242, 173-195.
- Simo, J.C. and Hughes, T. (1986), "On the variational foundation of assumed strain methods", *ASME J. Appl. Mech.*, **53**, 51-54.
- Srinivasan, K.R., Matous, K. and Geubelle, P.H. (2008), "Generalized finite element method for modeling nearly incompressible bimaterial hyperelastic solids", *Comput. Meth. Appl. Mech. Eng.*, **197**, 4882-4893.
- Stenberg, R. (1990), "Error analysis of some finite element methods for the Stokes problem", *Math. Comput.*, **54**, 495-508.
- Stevenson, A.C. (1943), "Some boundary problems of two-dimensional elasticity", *Philos. Mag.*, **34**, 766-793.
- Vidal, Y., Villon, P. and Huerta, A. (2003), "Locking in the incompressible limit: pseudo-divergence-free element free Galerkin", *Commun. Numer. Meth. Eng.*, **19**, 725-735.
- Washizu, K. (1982), *Variational Methods in Elasticity and Plasticity (3rd edn)*, Pergamon Press, New York.
- Wu, C.T. and Koishi, M. (2009), "A meshfree procedure for the microscopic analysis of particle-reinforced rubber compounds", *Interact. Multiscale Mech.*, **2**, 147-169.
- Wu, C.T., Park, C.K. and Chen, J.S. (2011), "A generalized meshfree approximation for the meshfree analysis of solids", *Comput. Meth. Appl. Mech. Eng.*, **85**, 693-722.
- Wu, C.T. and Hu, W. (2011), "Meshfree enriched simplex elements with strain smoothing for the finite element analysis of compressible and nearly incompressible solids", *Comput. Meth. Appl. Mech. Eng.*, **200**, 2991-3010.
- Wu, C.T. and Hu, W. (2012), "A two-level mesh repartitioning scheme for the displacement-based lower-order finite element methods in volumetric locking-free analyses", *Comput. Mech.*, **50**, 1-18.
- Yang, B., Laursen, T.A. and Meng, X. (2005), "Two dimensional mortar contact methods for large deformation frictional sliding", *Comput. Meth. Appl. Mech. Eng.*, **62**, 1183-1225.
- Zienkiewicz, O.C. and Taylor, R.L. (1987), *The finite element method (third ed.)*, McGraw-Hill, London.